ACS APPLIED MATERIALS & INTERFACES

RESEARCH ARTICLE

www.acsami.org

Protein-Repellent Silicon Nitride Surfaces: UV-Induced Formation of Oligoethylene Oxide Monolayers

Michel Rosso,[†,‡,§] Ai T. Nguyen,[†,§] Ed de Jong,[†] Jacob Baggerman,[†] Jos M. J. Paulusse,[†] Marcel Giesbers,[†] Remko G. Fokkink,[⊥] Willem Norde,[⊥] Karin Schroën,[‡] Cees J. M. van Rijn,[†] and Han Zuilhof*[,†]

[†]Laboratory of Organic Chemistry, Wageningen University, Dreijenplein 8, 6703 HB Wageningen, The Netherlands

[‡]Laboratory of Food and Bioprocess Engineering, Wageningen University, Bomenweg 2, 6703 HD Wageningen, The Netherlands

[⊥]Laboratory of Physical Chemistry and Colloid Science, Wageningen University, Dreijenplein 6, 6703 HB Wageningen, The Netherlands

Supporting Information

ABSTRACT: The grafting of polymers and oligomers of ethylene oxide onto surfaces is widely used to prevent nonspecific adsorption of biological material on sensors and membrane surfaces. In this report, we show for the first time the robust covalent attachment of short oligoethylene oxide-terminated alkenes ($CH_3O(CH_2CH_2O)_3(CH_2)_{11}$-$(CH{=}CH_2)$ [EO_3] and $CH_3O(CH_2CH_2O)_6(CH_2)_{11}$-$(CH{=}CH_2)$ [EO_6]) from the reaction of alkenes onto silicon-rich silicon nitride surfaces at room temperature using UV light. Reflectometry is used to monitor in situ the nonspecific adsorption of bovine serum albumin (BSA) and fibrinogen (FIB) onto oligoethylene oxide coated silicon-rich silicon nitride surfaces (EO_n-Si_xN_4, $x > 3$) in comparison with plasma-oxidized silicon-rich silicon nitride surfaces (SiO_y-Si_xN_4) and hexadecane-coated Si_xN_4 surfaces (C_{16}—Si_xN_4). A significant reduction in protein adsorption on EO_n-Si_xN_4 surfaces was achieved, adsorption onto EO_3—Si_xN_4 and EO_6—Si_xN_4 were 0.22 mg m^{-2} and 0.08 mg m^{-2}, respectively. The performance of the obtained EO_3 and EO_6 layers is comparable to those of similar, highly protein-repellent monolayers formed on gold and silver surfaces. EO_6—Si_xN_4 surfaces prevented significantly the adsorption of BSA (0.08 mg m^{-2}). Atomic force microscopy (AFM), X-ray photoelectron spectroscopy (XPS), X-ray reflectivity and static water contact angle measurements were employed to characterize the modified surfaces. In addition, the stability of EO_6—Si_xN_4 surfaces in phosphate-buffered saline solution (PBS) and alkaline condition (pH 10) was studied. Prolonged exposure of the surfaces to PBS solution for 1 week or alkaline condition for 2 h resulted in only minor degradation of the ethylene oxide moieties and no oxidation of the Si_xN_4 substrates was observed. Highly stable antifouling coatings on Si_xN_4 surfaces significantly broaden the application potential of silicon nitride-coated microdevices, and in particular of microfabricated filtration membranes.

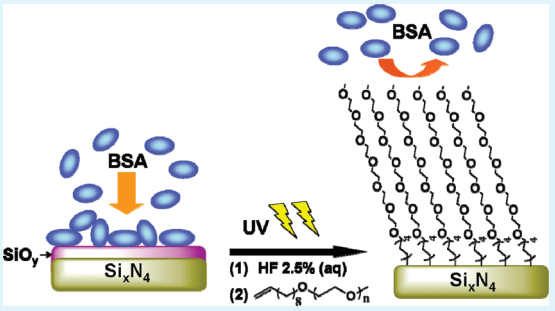

KEYWORDS: silicon nitride, UV-induced organic monolayers, oligoethylene oxide, reflectometry, protein-repelling surfaces

1. INTRODUCTION

Silicon nitride (Si_xN_4, $x \geq 3$) is widely used as insulator for microelectronics and microsystem devices.[1] Films of this material inhibit diffusion of water, oxygen and sodium ions and are widely used as passivation layers in integrated circuits.[2] Si_xN_4 is not only popular because of its superior physical robustness and chemical inertness,[3] but also because it provides a good alternative to silicon dioxide[4] in microelectronic and membrane applications.[5−7]

Biocompatibility is an important issue for the use of Si_xN_4 films as coatings for biosensors or filtration membranes. In particular, the performance of microfabricated filtration membranes (microsieves) is dramatically affected by nonspecific adsorption of protein (aggregates)[8,9] on surfaces during filtration. In the process of surface fouling, the adsorption of the first protein layer is a decisive step that usually initiates surface contamination, creating suitable conditions for the subsequent adsorption of more protein aggregates,[10] as well as cells, bacteria, and other microorganisms.[11]

Increasing the hydrophilicity of Si_xN_4 surfaces partially solves the problem of protein adsorption. Indeed, hydrophilic membranes are less subject to fouling and have a longer operational life.[12−14] An air-based plasma treatment, for instance, that superficially oxidizes the silicon nitride surfaces, can improve the wettability and performance of membranes. However, the hydrophilic properties of oxidized surfaces are only temporary.[15]

Widely used alternative solutions to reduce protein adsorption onto surfaces include self-assembled monolayers (SAMS) of ethylene oxide (EO) oligomers. This approach has been applied

Received: October 12, 2010
Accepted: January 20, 2011
Published: February 10, 2011

to polymers,[16−21] gold and silver,[22−30] glass and other oxides,[31−39] and etched silicon surfaces.[19,40−44] The application to silicon nitride would require a method for the robust attachment of such EO-based materials. Several studies reported on the specific modification of AFM tips[45−50] with polyethylene oxide chains, for applications in which only a few attached chains sufficed. Some work has been carried out on the attachment of long polyethylene oxide chains on oxidized silicon nitride,[51] but these irregular coatings were not stable in water. Organosilane compounds have been used to graft polyethylene oxide methacrylate[52] onto oxidized silicon nitride, giving layers with some protein-repellent properties, but the obtained layers were not stable under aqueous or alkaline conditions, most likely because of the hydrolysis of Si−O bonds.[51,53] Another report on organosilane-based monolayers of linear oligoethylene oxide molecules [3 - 12 ethylene oxide (EO) units] on oxidized silicon nitride substrates[54] also mentioned good thermal stability, but details on their hydrolytic stability or protein repellence were not given. Recently, we have shown that it is possible to covalently attach an organic monolayer onto a silicon nitride[55,56] or silicon carbide[57] surface, using conditions similar to those used for the thermal hydrosilylation of silicon surfaces.[58−61] Stable and high-quality monolayers were obtained with several simple alkenes, as well as esters, allowing further (bio)chemical surface modifications. However, the employed reaction conditions were not suitable for attachment of oligoethylene oxide because of thermal degradation of ethylene oxide moieties.[62] Very recently, it was demonstrated that the modification of SiO_2, Si_xN_4 and SiC can also be initiated by UV light at room temperature using less compound and a simpler experimental setup.[63−65] This method allows monolayer formation from labile and/or more expensive alkenes.

In the current paper, we report on the use of this photochemical method to attach oligoethylene oxide-terminated monolayers onto silicon-rich silicon nitride surfaces in a single-step procedure. In particular, methoxy-tri(ethylene oxide) undec-1-ene ($CH_3O(CH_2CH_2O)_3(CH_2)_9CH{=}CH_2$), and methoxy-hexa(ethylene oxide) undec-1-ene ($CH_3O(CH_2CH_2O)_6(CH_2)_9CH{=}CH_2$) were synthesized and grafted onto etched silicon-rich silicon nitride (Si_xN_4) surfaces, to yield monolayers abbreviated as EO_3 and EO_6 layers, respectively. The obtained monolayers were characterized by X-ray photoelectron spectroscopy (XPS), static water contact angle measurements, X-ray reflectivity, and atomic force microscopy (AFM). Subsequently, the protein-repelling properties of the surfaces were investigated by studying the adsorption of bovine serum albumin (BSA) and fibrinogen (FIB) from solution, both in situ by reflectometry and ex situ by static water contact angle measurement. In each case, the antifouling properties of modified surfaces were compared to those of SiO_y-Si_xN_4 and C_{16}-Si_xN_4 surfaces to reveal the potential of EO_3 and EO_6 monolayers. The stability of modified surfaces in aqueous solutions plays an important role for their future implementation in filtration and microfluidic devices. Therefore, the stability of the EO_6-modified surfaces in PBS solutions was investigated as well.

2. EXPERIMENTAL SECTION

Materials. Bovine serum albumin (fraction V, min 96% lyophilized powder) and fibrinogen (fraction I from pig plasma, 78% in protein) were purchased from Sigma. Sodium phosphate dibasic (analytical grade, Acros), potassium dihydrogenophosphate (ACS grade, Merck), potassium chloride (pro analysis, Merck) and sodium chloride (puriss., Riedel-de-Haën) were used to prepare the PBS solution.

Silicon Nitride Surface Modification. Silicon-rich silicon nitride samples (CVD Si_xN_4, $x > 3$) on Si(100), thickness of 147 nm, obtained from Lionix B.V., The Netherlands, with sizes of 1×1 cm^2 for XPS or 4×0.75 cm^2 for reflectometry were cleaned by sonication in acetone, followed by oxidation in air-based plasma for 10 min and in pure oxygen (99.999%) for another 5 min. The oxidized samples were then etched with a 2.5% aqueous solution of HF for 2 min and dried in a nitrogen flow. They were then immediately dipped into argon-saturated neat alkenes in a quartz flask. After 30 more min under argon flow, a UV pen lamp (254 nm, low pressure mercury vapor, double bore lamp from Jelight Cie, California) was placed 4 mm above the Si_xN_4 surface and the sample was irradiated for 24 h. Afterward, samples were removed and rinsed several times with ethyl acetate, ethanol and dichloromethane, and sonicated in the same solvents. Reference hydrophilic surfaces were plasma-treated for only 10 min. Angle-resolved XPS revealed that such plasma-treated surfaces presented a thin hydrophilic layer of silicon oxynitride (Atomic composition of the first 10 nm: 40% Si_{2p}, 30% N_{1s}, 20% O_{1s}, 10% C_{1s}, values obtained from XPS ± 5%).

Static Water Contact Angle Measurements. The wetting properties of modified surfaces were characterized by automated static water contact angle measurements performed using an Erma Contact Angle Meter G-1 (volume of the drop of demineralized water = 3.5 μL). For stability measurements, samples were dipped in PBS for a defined time and then rinsed thoroughly with pure water, acetone and finally with petroleum ether before measuring contact angle. After that, the samples were immersed again in fresh PBS. Stability for different times was determined sequentially on the same samples. For the stability in alkaline condition, the samples were immersed in NaOH solution (pH 10) at room temperature for 2 h, subsequently rinsed thoroughly with pure water, acetone, and finally with petroleum ether before measuring contact angle. In both studies, 3 samples were employed, the reported data were average value.

X-ray Photoelectron Spectroscopy (XPS). The XPS analysis of surfaces was performed using a JPS-9200 Photoelectron Spectrometer (JEOL, Japan). The high-resolution spectra were obtained under UHV conditions using monochromatic Al K_α X-ray radiation at 12 kV and 25 mA, using an analyzer pass energy of 10 eV. High-resolution spectra were corrected with a linear background before fitting.

X-ray Reflectivity. X-ray reflectivity measurements were performed on a Panalytical X′Pert Pro diffractometer using nickel-filtered Cu K_α radiation (tube settings 50 kV and 40 mA). The data were collected using a fixed divergence slit 1/32°, and a parallel plate collimator on the diffracted beam side. The layer thickness was calculated from the interference fringes.

Atomic Force Microscopy (AFM). Images were obtained with an MFP-3D AFM from Asylum Research (Santa Barbara, CA). Imaging was performed in AC mode in air using OMCL-AC240 silicon cantilevers (Olympus Corporation, Japan). The root-mean-square (rms) roughness was calculated from the fluctuations of the surface height around the average height in the image. In this way the rms value describes the topography of the surface. The rms is the standard deviation, i.e. the square root of the variance, of the Z-values within the image, according to: rms = $\sqrt{(\sum(Z_i)^2/n)}$

Reflectometry. In a typical reflectometer, a monochromatic linearly polarized light beam (He−Ne laser; 632.8 nm) passes a 45° glass prism. This beam arrives at the interface with an angle of incidence of 66° for the solvent/substrate interface. After reflection at the interface and refraction in the prism the beam is split into its p- and s-polarized components relative to the plane of incidence by means of a beam splitter. Both components are separately detected by two photodiodes and the ratio between the intensity of the parallel and perpendicular components is the output signal S ($S = I_p/I_s$) (the output signal given by the detection box is $10 \times S$). It is combined with a stagnation point flow cell, allowing the introduction of PBS solution or protein solutions, to

study homogeneous adsorption on surfaces in diffusion-controlled conditions.[66] Strips of Si_xN_4-coated silicon wafer (typical size of 4 × 0.75 cm^2) were modified with alkenes on one end (about half of the sample length), whereas the other end was used to hold the strip in the measuring cell of the reflectometer. The BSA solutions (0.1 g L^{-1}) were freshly prepared in PBS solution (pH 6.75, ionic strength 0.08 M) and settled for one hour at room temperature before use in measurement. Due to a lower solubility in water, FIB solutions were prepared differently. First, PBS solution at pH 6.7 with a higher ionic strength of 0.16 M was prepared. The desired amount of FIB was added and the solution was gently shaken at 80 rpm at room temperature during 15 min to obtain a clear protein solution. Finally, the solution was diluted with water to obtain 0.1 g L^{-1} of FIB in PBS solution at pH 6.7 with ionic strength 0.08M. All reflectometry experiments were performed at 23 °C. Before measurements were taken, surfaces were incubated 1 h in PBS solution to avoid artifacts due to initial surface wetting, which caused a baseline drift. After placing the samples in the reflectometer, the PBS solution was injected until the output signal was nearly constant: fluctuations of less than 1% over 5 min were considered satisfactory. Each experiment involved at least one adsorption phase, in which protein solutions were injected onto the surface, and one subsequent desorption phase, in which only PBS solution was injected. Details of the calculation of adsorbed protein amount are given in the Supporting Information. Each experiment was repeated at least 3 times, and the reported data are average values.

3. RESULTS AND DISCUSSION

3.1. Silicon Nitride Surface Modification with EO_3 and EO_6. Silicon nitride was functionalized in a one-step photochemical procedure as described in the Experimental Section. Hydrogen-terminated Si_xN_4 surfaces were obtained by etching with HF, and the surfaces were subsequently employed in the photochemical attachment of $CH_3O(CH_2CH_2O)_3(CH_2)_9CH{=}CH_2$ [EO_3] and $CH_3O(CH_2CH_2O)_6(CH_2)_9CH{=}CH_2$ [EO_6]. Under UV irradiation, the double bonds readily react with silicon atoms on the hydrogen-terminated surface resulting in Si−C linkages. The resultant UV-modified Si_xN_4 surfaces with covalently attached EO_3 and EO_6 monolayers exhibited very reproducible static water contact angles of 64° and 58° (±1°), respectively, in agreement with previous reports on similar monolayers on other surfaces. Water contact angles of EO_3-modified Si_xN_4 surfaces (64° ± 1°) are identical to those measured for EO_3 monolayers obtained with thiols on gold and silver,[30] but lower values were obtained for EO_3 monolayers obtained by reaction of alkenes with hydrogen-terminated silicon (58 ± 1°).[40,44] In general, substrates coated with EO_3 monolayers display water contact angle values smaller than 11-methoxyundecene thiol monolayers on gold surfaces (∼84°),[28,67] suggesting that internal ether bonds of the ethylene oxide moieties are always partially exposed. EO_6 coatings on Si_xN_4 were even more hydrophilic, with a contact angle of 58° ± 1°, which is between the values of 66° and 49 ± 1° observed for EO_6 monolayers on gold[29] and silicon[40] surfaces, respectively. The hydrophilic character of modified surfaces correlates with the disorder and the packing density of oligo-ethylene oxide monolayers, exposing polar internal C−O bonds to the outer environment. It can thus be concluded that EO_3 monolayers on Si_xN_4 are comparable to thiol monolayers on gold or silver, while EO_6 monolayers on Si_xN_4 are slightly less densely packed.

It was attempted to measure this difference in density and the resulting thickness by X-ray reflectivity measurements. The thus obtained thicknesses for both types of monolayers is 2.6 ± 0.2 nm, which would correspond to 95 and 70% of the length of extended EO_3 and EO_6 molecules, respectively. However, beside the 0.2 nm uncertainty associated with the reflectivity measurement, the initial roughness of bare amorphous Si_xN_4 surfaces obtained by AFM (0.45 ± 0.05 nm for all surfaces used; see Table 1) yields an uncertainty of 0.6 nm. This brings these thicknesses obtained by X-ray reflectivity into inconclusive to identify EO_3 and EO_6 monolayer, and thus hampers a direct comparison with reported values for EO_3 and EO_6 monolayers on gold surfaces (2.0 ± 0.2 and 2.8 ± 0.2 nm,[28] respectively).

Table 1. RMS Roughness Measured by AFM on Oxidized Si_xN_4 and on EO_n-coated Si_xN_4, before and after Exposure to Protein Solution (values are ±0.05 nm)

samples	before adsorption (nm)	after BSA adsorption (nm)	before adsorption (nm)	after FIB adsorption (nm)
oxidized Si_xN_4	0.48	0.81	0.49	0.80
Si_xN_4-EO_3	0.49	0.57	n.d.	n.d.
Si_xN_4-EO_6	0.45	0.52	0.40	0.44

The C_{1s} regions of the XPS data measured on EO_3 and EO_6 monolayers (Figure 1) display the two characteristic peaks corresponding to carbon of the hydrocarbon chains (C−C at 285.0 eV) and oxygen-bound carbon (C−O at 286.8 eV). After fitting the high-resolution spectra, the measured (C−C)/(C−O) ratios of 1.30 (EO_3 coatings) and 0.77 (EO_6 coatings) are close to the theoretical stoichiometry values of 1.25 (10/8) and 0.71 (10/14), showing the intact attachment of the EO alkenes. Similar attachment experiments at elevated temperatures lead to cleavage of the EO moieties, showing the necessity of this mild attachment with light.

The AFM images of coated substrates (Figure 2) show a typical clean Si_xN_4 surface after oxidation (left), and two analogous surfaces coated with EO_3 (center) and EO_6 (right) monolayers. Images and profile traces appear identical before and after modification, still displaying the structure of the initial Si_xN_4 substrate, with only marginal sample-to-sample variation.

From these characterizations (water contact angle, XPS, AFM and X-ray reflectivity) it can be concluded that by using UV irradiation homogeneous EO_3 and EO_6 monolayers on silicon nitride surfaces are obtained reproducibly. Moreover these monolayers display comparable features as observed earlier for such monolayers on silicon and gold surfaces. However, the higher stability of these coatings on Si_xN_4 makes them preferred for applications where long-term stability of surfaces is required.[55,56,64]

3.2. Protein Adsorption onto Modified Si_xN_4 Surfaces. In contrast to all the ex situ techniques used to monitor protein adsorption onto surfaces (e.g., contact angle, AFM, XPS, ellipsometry, quartz micro balance), reflectometry allows in situ observation of protein adsorption without removing the surface from the protein solution and without intermediate cleaning steps. In addition, this allows one to distinguish between reversible and irreversible adsorption during the adsorption and rinsing phases, respectively. Air-based plasma oxidized surfaces (SiO_y-Si_xN_4) were used as references in our protein adsorption survey. Other studies have reported protein-repellent behavior by comparison with methyl-terminated surfaces, obtained by formation of alkyl monolayers on silicon[44] or gold surfaces.[28] In fact, such hydrophobic surfaces adsorb significantly more protein in aqueous solution, compared to hydrophilic surfaces, to minimize interfacial tension

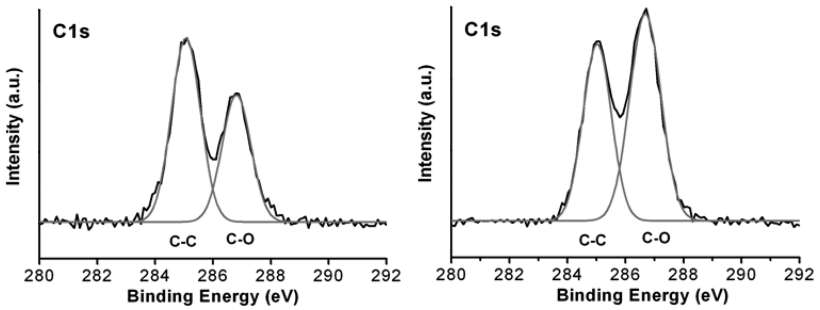

Figure 1. XPS narrow-scan spectra of C_{1s} region of Si_xN_4 ($x \approx 4$) surfaces coated with ethylene oxide-containing monolayers. Left: monolayer of $CH_3O(CH_2CH_2O)_3(CH_2)_{11}$ [EO_3]; right: monolayer of $CH_3O(CH_2CH_2O)_6(CH_2)_{11}$ [EO_6].

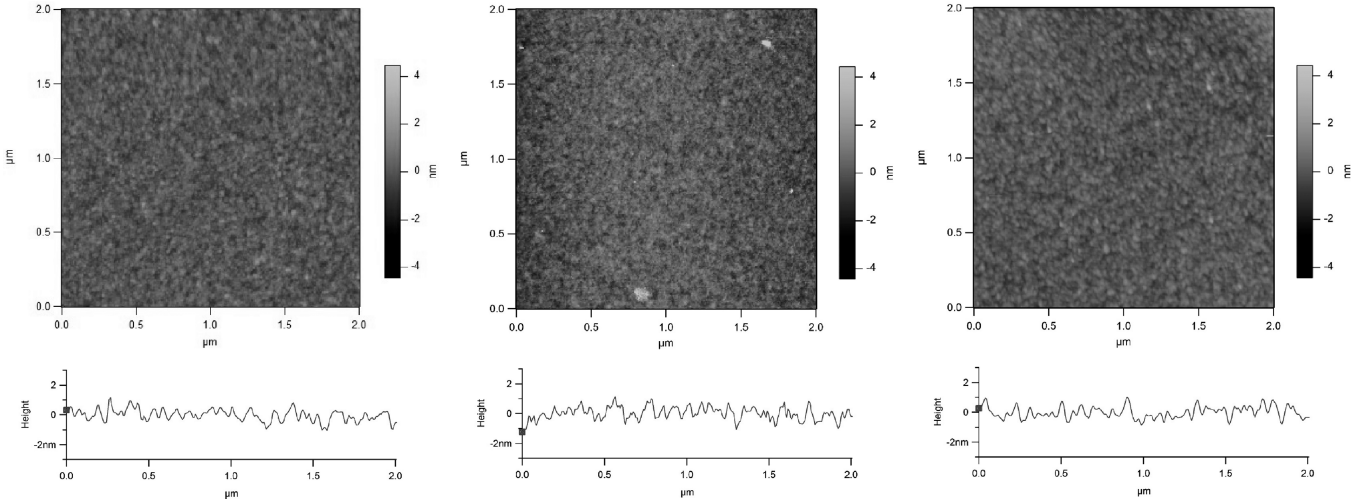

Figure 2. AFM images of oxidized (left), EO_3-coated (center), and EO_6-coated (right) Si_xN_4 surfaces and corresponding profile traces. Horizontal scale of images, 2 μm; height scale, 8.8 nm. Profile height scale, 6 nm.

between coatings and water phase. In comparison, the hydrophilic surfaces, which have a higher surface energy, have a low interfacial energy with water; as a result, it is less favorable for proteins to adsorb on the surfaces, i.e., the surfaces repel proteins.[68] In agreement with these earlier observations, our experimental results showed that the protein adsorption onto hydrophobic hexadecane-coated Si_xN_4 surfaces (C_{16}-Si_xN_4) is much higher than that of SiO_y-Si_xN_4 surfaces. The adsorption of FIB on C_{16}-Si_xN_4 surfaces was 91% higher than on SiO_y-Si_xN_4 surfaces and 12% higher for BSA. These results show that the adsorption of proteins onto hydrophobic and hydrophilic surfaces differs significantly depending on the type of protein, and in the case of monolayer-modified surfaces will likely vary with the quality of the monolayer. Therefore, the use of hydrophilic SiO_y-Si_xN_4 surfaces as reference allowed us to have a stricter comparison in the efficiency of the protein repellence of hydrophilic EO coatings.

When exposed to protein solutions, the SiO_y-Si_xN_4 surfaces showed a reproducible maximum adsorbed amount of 1.25 ± 0.1 mg m^{-2} of BSA, and 3.0 ± 0.1 mg m^{-2} of FIB (Figure 3). There was no desorption during cleaning with PBS solution, showing that the adsorption is almost entirely irreversible. The difference in the maximum adsorbed amounts of FIB and BSA on SiO_y-Si_xN_4 surfaces are partially due to differences in the charges on the proteins. The pI value of FIB is 6.0, which indicates that FIB is nearly neutral at pH 6.7. In contrast, BSA has a pI value of 4.7, showing that BSA is negatively charged in PBS solution. Thus, BSA has difficulties to approach the surface due to repulsive electrostatic forces at the negatively charged SiO_y-Si_xN_4 surfaces (pI = 1.7−3.5),[69] leading to a low adsorption rate. Once the protein has attached to the surface, it relaxes toward a (set of) new equilibrium structure(s) to optimize the protein−surface interaction. This normally involves a certain degree of spreading of the protein over the surface, creating more contacts with the surface.[70] As a consequence, it will be less favorable for the next protein to adhere. This results in a low maximum adsorbed amount of BSA on SiO_x-Si_xN_4. In comparison, FIB can more easily approach the surface due to the neutrality of the protein under our experimental conditions. Thus, it adsorbs onto the surface with a higher adsorption rate, leading to early full occupation on the surfaces (plateau region). This leaves less space for the protein to spread out on the surface. The data shows that the adsorption can reach the plateau region corresponding to saturated occupation of the surface within 3 min in the case of FIB and 20 min for BSA (see Figure S2 in Supporting Information).

The adsorbed amount of BSA on EO_3−Si_xN_4 was 0.22 mg m^{-2}, corresponding to 82% repellence compared to SiO_y-Si_xN_4. Water contact angle measurements on the exposed surfaces revealed similar values, most likely due to the adhesion of small amounts of protein (Figure 4). Remarkably, EO_6−Si_xN_4 surfaces only adsorbed 0.08 mg m^{-2}, corresponding to 94% repellence. These results demonstrate the important role of the length of ethylene oxide chain in the repulsion of proteins. Our experimental data is in agreement with the results of Grunze and co-workers on similar work on gold surfaces about protein repellence of EO_n coatings,[29]

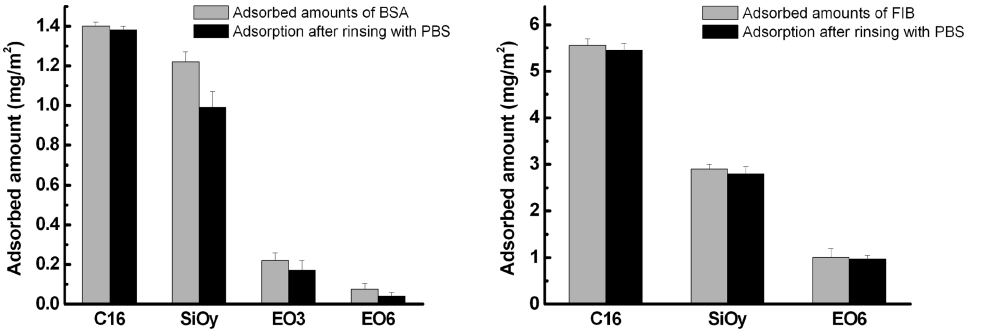

Figure 3. Reflectometry data: adsorbed amounts of BSA (left) and FIB (right) onto hexadecane-coated Si_xN_4 (C_{16}), plasma-oxidized Si_xN_4 (SiO_y), and EO_3/EO_6-coated Si_xN_4 surfaces (EO_3 and EO_6), after subsequent exposure to protein solution and to PBS solution.

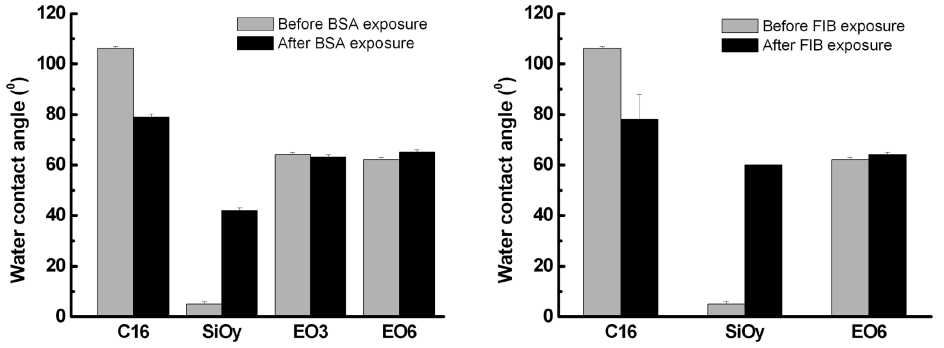

Figure 4. Static water contact angles values before and after adsorption of BSA (left) and FIB (right) onto hexadecane-coated Si_xN_4 (C_{16}), plasma-oxidized Si_xN_4 (SiO_y) and EO_3/EO_6-coated Si_xN_4 surfaces (EO_3 and EO_6), after subsequent exposure to protein solution and to PBS solution.

and with several simulation studies on the role of hydration layers in protein repellent coatings.[71−73] A longer chain of ethylene oxide results in a thicker hydrophilic part within the coating, which plays a crucial role in the repellence of proteins. As EO_6-Si_xN_4 coated surfaces gave a better protein repellent property compared to EO_3−Si_xN_4 surfaces, we used EO_6-Si_xN_4 surfaces to study the behavior of ethylene oxide chain with different protein, i.e., FIB and its stability.

Higher adsorbed amounts of FIB were observed on EO_6−Si_xN_4 modified surfaces (1 ± 0.05 mg m^{-2}) as compared to BSA, corresponding to 67% repellence by the modified surface, with water contact angle values of these EO_6-Si_xN_4 surfaces that were the same before and after exposure to protein solution. This latter observation can be attributed to similarity in hydrophilicity between EO_n-modified surfaces and adsorbed protein layer as explained earlier. The adsorption of FIB on C_{16}-Si_xN_4 and SiO_x-Si_xN_4 surfaces was also considerably higher than BSA, 5.6 and 2.9 mg m^{-2}, respectively. FIB is a fibrous protein (MW = 340 kDa) with dimensions of about $9 \times 9 \times 45$ nm^3,[74] and has a weak internal cohesion. In comparison, BSA is a globular protein (MW = 69 kDa) with dimensions of $4 \times 4 \times 14$ nm^3,[75] having a compact structure and stronger cohesion, which is less favorable as compared to FIB for the structural rearrangement when proteins absorb onto a surface.[76] This is supported by DLVO theory, which describes the forces between interacting surfaces through a liquid medium.[77] A calculation of the van der Waals interactions between proteins (FIB and BSA) and monolayer-modified surfaces indicates that the interaction between FIB and the surface is approximately 4 times greater than the energy of thermal motion, whereas the van der Waals interaction between BSA and the surface is only half the energy of thermal

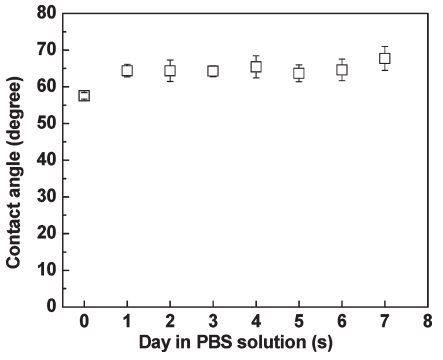

Figure 5. Static water contact angle of EO_6−Si_xN_4 surfaces exposed to PBS solution for 1 week.

motion (see the Supporting Information). These results are in agreement with the experimental finding of a higher adsorption rate for FIB as compared to BSA.

In addition, we noticed that the preparation of the FIB solution influenced the total adsorbed amount of protein, whereas its adsorption onto SiO_y-Si_xN_4 surfaces was approximately the same as in the case of FIB solution prepared as described in the Experimental Section. A thick foam layer on top of the protein solution formed during shaking and remained even after settling for one hour at room temperature. As a result, the obtained concentration in bulk solution was likely significantly reduced. Furthermore, this procedure probably causes denaturation of proteins, leading to changes in protein conformation and thus in the adsorption behavior of the proteins onto the surface. Finally, shaking caused the adsorbed amount of FIB onto EO_6−

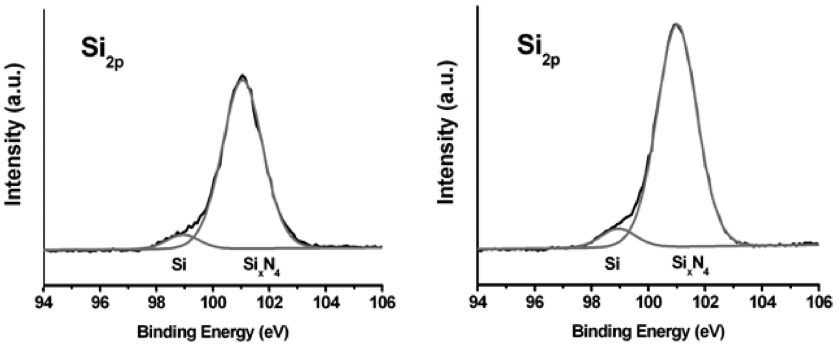

Figure 6. XPS narrow-scan spectra of Si_{2p} region of $EO_6-Si_xN_4$ surfaces before exposure (left) and after exposure (right) to PBS solution for 1 week.

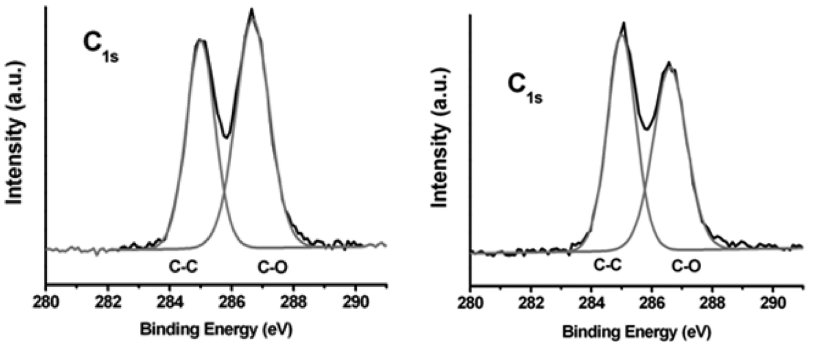

Figure 7. XPS narrow-scan spectra of C_{1s} region of $EO_6-Si_xN_4$ surfaces before exposure (left) and after exposure (right) to PBS solution for 1 week.

Si_xN_4 surfaces to become irreproducible. In comparison, dissolving FIB gently at higher ionic strength resulted in homogeneous solutions without foam,[78] i.e., a desired amount of FIB was dissolved in high ionic strength PBS solution (I = 0.16M), subsequently the solution was diluted with water to obtain 0.08 M ionic strength PBS solution, and finally gently shaken (80 rpm) at room temperature for 15 min to obtain homogeneous solution. A very reproducible maximum adsorbed amount was achieved when the protein was dissolved gently.

3.3. Stability of Modified Si_xN_4 Surfaces in Aqueous Media. The stability of antifouling poly(ethylene oxide) coatings immobilized onto silicon substrates via organosilane chemistry has been investigated by several research groups.[53,79−81] Ethylene oxides are known to degrade upon exposure to water, and an auto-oxidation mechanism has recently been reported by Qin et al.[79] Monolayer degradation is a complex process, which depends on the nature and chemical stability of the monolayer molecules, the type of connection between the modified layer and the substrate, as well as the packing density and ordering of the immobilized molecules. However, prolonged stability studies were not performed. The usefulness of functionalized surfaces hinges for many applications around the stability of that functionalization upon long-term exposure to aqueous solutions. We therefore studied the stability of the EO_6-monolayers on silicon nitride surfaces in PBS during 1 week. Static water contact angles were measured daily, and the results are depicted in Figure 5. A slight increase in contact angle (~6°) was measured after the first day, but no significant changes were observed during the following days. XPS measurements were performed before and after exposure to PBS. After 7 days in PBS, the wide-scan XPS spectra of modified silicon nitride substrates revealed a decrease in the C/Si ratio from 1.09 to 0.75 (31 ± 3%). The XPS narrow-scan of the C_{1s} region showed a reduction of the C−O signal at 286.7 eV, and a decrease in the C−O/C−C ratio from 1.25 to 0.99 (20 ± 3%), which corresponds approximately to an average of 1 unit of ethylene oxide being cleaved off (Figure 6, 7). This cleavage is attributed to auto-oxidation of ethylene oxide moieties.[79,80] This minor degradation is most likely the reason for the change in contact angle that was observed. Interestingly, in the XPS narrow-scan spectrum of the Si_{2p} region, no oxidation of the exposed substrates was observed, demonstrating the robustness of the Si−C linkage.

After a week in PBS, the majority of the ethylene oxide segments are still intact, and so the monolayer should also still be able to repel proteins. The protein repellency of the exposed EO_6-coated surfaces was therefore investigated, and reflectometry measurements revealed that the maximum adsorbed amount of BSA on the exposed surface was 0.44 ± 0.05 mg m^{-2}. In other words: even after exposure of a week to PBS solution, 65% of BSA was still repelled, as compared to plasma-oxidized silicon nitride surfaces.

Recently, Sano et al. reported on the stability of monolayers bound onto Si (111) surfaces via Si−C and Si−O−C bonds in various basic and acidic media during 1 h.[53] The Si−C bound monolayers showed superior stability compared to monolayers bound via Si−O−C linkages. To determine the application potential of the modified surfaces, the stability of the EO_6 modified Si_xN_4 surfaces was further studied in alkaline condition (pH 10) at room temperature for 2 h. Static water contact angle measurements and XPS were used to characterize the surfaces before and after the stability study. No significant change in water contact angle value was observed. The ratio of C/Si derived from the wide-scan XPS spectra changed only to a minor degree, within error of measurement. The narrow-scan XPS spectrum of

the C_{1s} region, however, showed cleavage of 1.5 EO units (on average) from the oligo(ethylene oxide) chain. The narrow-scan XPS spectrum of the Si_{2p} region did not show a silicon oxide peak at 104 eV (see Figure S3 in the Supporting Information). These results indicate that the degradation mainly occurs at the ethylene oxide chain due to auto-oxidation as mentioned before, whereas the Si−C linkage remains intact not only in PBS solution but also under alkaline conditions.

4. CONCLUSIONS

For the first time, well-defined monolayers of short oligoethylene oxide chains, $CH_3O(CH_2CH_2O)_3(CH_2)_{11}$ [EO_3] and $CH_3O(CH_2CH_2O)_6(CH_2)_{11}$ [EO_6] were successfully grafted onto silicon-enriched Si_xN_4 surfaces using a photochemical attachment of 1-alkenes at room temperature.[64] Such EO_n-modified Si_xN_4 surfaces displayed excellent protein-repelling behavior. EO_6 monolayers reduced the adsorption of proteins (FIB and BSA) significantly as compared to SiO_y-Si_xN_4. In addition, a strong dependence on the dissolution method of FIB on the adsorption efficiency was found. Investigations into the stability of EO_6−Si_xN_4 surfaces revealed minor degradation of the ethylene oxide moieties upon exposure to PBS for 1 week, as well as upon exposure under alkaline conditions (pH 10) for 2 h, whereas no oxidation of the substrate was observed. The inertness of the silicon nitride substrate and the robust Si−C linkage through which the monolayers are coupled provide for highly stable substrates. The excellent antifouling behavior combined with the high stability of these monolayers opens up a wide range of practical applications, such as in reactor walls, biosensors, or lithographically prepared microsieves.

■ ASSOCIATED CONTENT

Supporting Information. The synthesis of EO_3 and EO_6 and calculation of adsorption amount of BSA and FIB onto surfaces (PDF). This material is available free of charge via the Internet at http://pubs.acs.org.

■ AUTHOR INFORMATION

Corresponding Author

*E-mail: Han.Zuilhof@wur.nl. Telephone: +31-317-482367. FAX: + 31-317-484914.

Author Contributions

§These authors contributed equally to this work.

■ ACKNOWLEDGMENT

The authors thank Graduate School VLAG and MicroNed (Project no. 6163510395 and no. 6163510587) for financial support.

■ REFERENCES

(1) Patil, L. S.; Pandey, R. K.; Bang, J. P.; Gaikwad, S. A.; Gautam, D. K. *Opt. Mater.* **2005**, *27*, 663–670.
(2) Bermudez, V. M.; Perkins, F. K. *Appl. Surf. Sci.* **2004**, *235*, 406–419.
(3) Antsiferov, V. N.; Gilev, V. G.; Karmanov, V. I. *Refract. Ind. Ceram.* **2003**, *44*, 108–114.
(4) Rathi, V. K.; Gupta, M.; Agnihotri, O. P. *Microelectron. J.* **1995**, *26*, 563.
(5) Kuiper, S.; van Wolferen, H.; van Rijn, C.; Nijdam, W.; Krijnen, G.; Elwenspoek, M. *J. Micromech. Microeng.* **2001**, *11*, 33–37.
(6) van Rijn, C. J. M.; Veldhuis, G. J.; Kuiper, S. *Nanotechnology* **1998**, *9*, 343–345.
(7) van Rijn, C. J. M., *Nano and Micro Engineered Membrane Technology*; Elsevier: Amsterdam, The Netherlands, 2004.
(8) Kuiper, S.; Brink, R.; Nijdam, W.; Krijnen, G. J. M.; Elwenspoek, M. C. *J. Membr. Sci.* **2002**, *196*, 149–157.
(9) Girones, M.; Lammertink, R. G. H.; Wessling, M. *J. Membr. Sci.* **2006**, *273*, 68–76.
(10) Marshall, A. D.; Munro, P. A.; Tragardh, G. *Desalination* **1993**, *91*, 65–108.
(11) Vanloosdrecht, M. C. M.; Lyklema, J.; Norde, W.; Zehnder, A. J. B. *Microbiol. Rev.* **1990**, *54*, 75–87.
(12) Koehler, J. A.; Ulbricht, M.; Belfort, G. *Langmuir* **2000**, *16*, 10419–10427.
(13) Ulbricht, M.; Belfort, G. *J. Appl. Polym. Sci.* **1995**, *56*, 325–343.
(14) Ulbricht, M.; Belfort, G. *J. Membr. Sci.* **1996**, *111*, 193–215.
(15) Girones, M.; Borneman, Z.; Lammertink, R. G. H.; Wessling, M. *J. Membr. Sci.* **2005**, *259*, 55–64.
(16) Amirgoulova, E. V.; Groll, J.; Heyes, C. D.; Ameringer, T.; Rocker, C.; Moller, M.; Nienhaus, G. U. *Chemphyschem* **2004**, *5*, 552–555.
(17) Bosker, W. T. E.; Iakovlev, P. A.; Norde, W.; Cohen Stuart, M. A. *J. Colloid Interface Sci.* **2005**, *286*, 496–503.
(18) Bremmell, K. E.; Kingshott, P.; Ademovic, Z.; Winther-Jensen, B.; Griesser, H. J. *Langmuir* **2006**, *22*, 313–318.
(19) Cecchet, F.; De Meersman, B.; Demoustier-Champagne, S.; Nysten, B.; Jonas, A. M. *Langmuir* **2006**, *22*, 1173–1181.
(20) Krishnan, S.; Ayothi, R.; Hexemer, A.; Finlay, J. A.; Sohn, K. E.; Perry, R.; Ober, C. K.; Kramer, E. J.; Callow, M. E.; Callow, J. A.; Fischer, D. A. *Langmuir* **2006**, *22*, 5075–5086.
(21) Lazos, D.; Franzka, S.; Ulbricht, M. *Langmuir* **2005**, *21*, 8774–8784.
(22) Yam, C. M.; Deluge, M.; Tang, D.; Kumar, A.; Cai, C. Z. *J. Colloid Interface Sci.* **2006**, *296*, 118–130.
(23) Vanderah, D. J.; Pham, C. P.; Springer, S. K.; Silin, V.; Meuse, C. W. *Langmuir* **2000**, *16*, 6527–6532.
(24) Unsworth, L. D.; Sheardown, H.; Brash, J. L. *Langmuir* **2005**, *21*, 1036–1041.
(25) Seigel, R. R.; Harder, P.; Dahint, R.; Grunze, M.; Josse, F.; Mrksich, M.; Whitesides, G. M. *Anal. Chem.* **1997**, *69*, 3321–3328.
(26) Prime, K. L.; Whitesides, G. M. *J. Am. Chem. Soc.* **1993**, *115*, 10714–10721.
(27) Prime, K. L.; Whitesides, G. M. *Science* **1991**, *252*, 1164–1167.
(28) Palegrosdemange, C.; Simon, E. S.; Prime, K. L.; Whitesides, G. M. *J. Am. Chem. Soc.* **1991**, *113*, 12–20.
(29) Herrwerth, S.; Eck, W.; Reinhardt, S.; Grunze, M. *J. Am. Chem. Soc.* **2003**, *125*, 9359–9366.
(30) Harder, P.; Grunze, M.; Dahint, R.; Whitesides, G. M.; Laibinis, P. E. *J. Phys. Chem. B* **1998**, *102*, 426–436.
(31) Chan, Y. H. M.; Schweiss, R.; Werner, C.; Grunze, M. *Langmuir* **2003**, *19*, 7380–7385.
(32) Heyes, C. D.; Kobitski, A. Y.; Amirgoulova, E. V.; Nienhaus, G. U. *J. Phys. Chem. B* **2004**, *108*, 13387–13394.
(33) Hoffmann, C.; Tovar, G. E. M. *J. Colloid Interface Sci.* **2006**, *295*, 427–435.
(34) Lee, S. W.; Laibinis, P. E. *Biomaterials* **1998**, *19*, 1669–1675.
(35) Ma, H. W.; Li, D. J.; Sheng, X.; Zhao, B.; Chilkoti, A. *Langmuir* **2006**, *22*, 3751–3756.
(36) Norde, W.; Gage, D. *Langmuir* **2004**, *20*, 4162–4167.
(37) Roosjen, A.; Kaper, H. J.; van der Mei, H. C.; Norde, W.; Busscher, H. J. *Microbiology* **2003**, *149*, 3239–3246.
(38) Roosjen, A.; van der Mei, H. C.; Busscher, H. J.; Norde, W. *Langmuir* **2004**, *20*, 10949–10955.
(39) Schlapak, R.; Pammer, P.; Armitage, D.; Zhu, R.; Hinterdorfer, P.; Vaupel, M.; Fruhwirth, T.; Howorka, S. *Langmuir* **2006**, *22*, 277–285.
(40) Yam, C. M.; Lopez-Romero, J. M.; Gu, J. H.; Cai, C. Z. *Chem. Commun.* **2004**, 2510–2511.

(41) Yam, C. M.; Gu, J. H.; Li, S.; Cai, C. Z. *J. Colloid Interface Sci.* **2005**, *285*, 711–718.
(42) Böcking, T.; Killan, K. A.; Gaus, K.; Gooding, J. J. *Langmuir* **2006**, *22*, 3494–3496.
(43) Böcking, T.; Kilian, K. A.; Hanley, T.; Ilyas, S.; Gaus, K.; Gal, M.; Gooding, J. J. *Langmuir* **2005**, *21*, 10522–10529.
(44) Böcking, T.; Gal, M.; Gaus, K.; Gooding, J. J. *Aust. J. Chem.* **2005**, *58*, 660–663.
(45) Ebner, A.; Wildling, L.; Kamruzzahan, A. S. M.; Rankl, C.; Wruss, J.; Hahn, C. D.; Holzl, M.; Zhu, R.; Kienberger, F.; Blaas, D.; Hinterdorfer, P.; Gruber, H. J. *Bioconjugate Chem.* **2007**, *18*, 1176–1184.
(46) Gabriel, S.; Jerome, C.; Jerome, R.; Fustin, C. A.; Pallandre, A.; Plain, J.; Jonas, A. M.; Duwez, A. S. *J. Am. Chem. Soc.* **2007**, *129*, 8410–8411.
(47) Gu, C.; Ray, C.; Guo, S.; Akhremitchev, B. B. *J. Phys. Chem. C* **2007**, *111*, 12898–12905.
(48) Kamruzzahan, A. S. M.; Ebner, A.; Wildling, L.; Kienberger, F.; Riener, C. K.; Hahn, C. D.; Pollheimer, P. D.; Winklehner, P.; Holzl, M.; Lackner, B.; Schorkl, D. M.; Hinterdorfer, P.; Gruber, H. J. *Bioconjugate Chem.* **2006**, *17*, 1473–1481.
(49) Riener, C. K.; Kienberger, F.; Hahn, C. D.; Buchinger, G. M.; Egwim, I. O. C.; Haselgrubler, T.; Ebner, A.; Romanin, C.; Klampfl, C.; Lackner, B.; Prinz, H.; Blaas, D.; Hinterdorfer, P.; Gruber, H. J. *Anal. Chim. Acta* **2003**, *497*, 101–114.
(50) Wang, T.; Xu, J. J.; Qiu, F.; Zhang, H. D.; Yang, Y. L. *Polymer* **2007**, *48*, 6170–6179.
(51) Suo, Z. Y.; Arce, F. T.; Avci, R.; Thieltges, K.; Spangler, B. *Langmuir* **2006**, *22*, 3844–3850.
(52) Girones, M.; Bolhuis-Versteeg, L.; Lammertink, R.; Wessling, M. *J. Colloid Interface Sci.* **2006**, *299*, 831–840.
(53) Sano, H.; Maeda, H.; Ichii, T.; Murase, K.; Noda, K.; Matsushige, K.; Sugimura, H. *Langmuir* **2009**, *25*, 5516–5525.
(54) Cerruti, M.; Fissolo, S.; Carraro, C.; Ricciardi, C.; Majumdar, A.; Maboudian, R. *Langmuir* **2008**, *24*, 10646–10653.
(55) Arafat, A.; Giesbers, M.; Rosso, M.; Sudhölter, E. J. R.; Schroën, K.; White, R. G.; Yang, L.; Linford, M. R.; Zuilhof, H. *Langmuir* **2007**, *23*, 6233–6244.
(56) Arafat, A.; Schroën, K.; de Smet, L. C. P. M.; Sudhölter, E. J. R.; Zuilhof, H. *J. Am. Chem. Soc.* **2004**, *126*, 8600–8601.
(57) Rosso, M.; Arafat, A.; Schroën, K.; Giesbers, M.; Roper, C. S.; Maboudian, R.; Zuilhof, H. *Langmuir* **2008**, *24*, 4007–4012.
(58) Ciampi, S.; Harper, J. B.; Gooding, J. J. *Chem. Soc. Rev.* **2010**, *39*, 2158–2183.
(59) Scheres, L.; Arafat, A.; Zuilhof, H. *Langmuir* **2007**, *23*, 8343–8346.
(60) Scheres, L.; Giesbers, M.; Zuilhof, H. *Langmuir* **2010**, *26*, 4790–4795.
(61) Scheres, L.; Giesbers, M.; Zuilhof, H. *Langmuir* **2010**, *26*, 10924–10929.
(62) Yang, L.; Heatley, F.; Blease, T. G.; Thompson, R. I. G. *Eur. Polym. J.* **1996**, *32*, 535–547.
(63) Qin, G.; Zhang, R.; Makarenko, B.; Kumar, A.; Rabalais, W.; Lopez Romero, J. M.; Rico, R.; Cai, C. *Chem. Commun.* **2010**, *46*, 3289–3291.
(64) Rosso, M.; Giesbers, M.; Arafat, A.; Schroën, K.; Zuilhof, H. *Langmuir* **2009**, *25*, 2172–2180.
(65) ter Maat, J.; Regeling, R.; Yang, M.; Mullings, M. N.; Bent, S. F.; Zuilhof, H. *Langmuir* **2009**, *25*, 11592–11597.
(66) Dijt, J. C.; Cohen Stuart, M. A.; Fleer, G. J. *Adv. Colloid Interface Sci.* **1994**, *50*, 79–101.
(67) Laibinis, P. E.; Bain, C. D.; Nuzzo, R. G.; Whitesides, G. M. *J. Phys. Chem.* **1995**, *99*, 7663–7676.
(68) Krishnan, S.; Weinman, C. J.; Ober, C. K. *J. Mater. Chem.* **2008**, *18*, 3405–3413.
(69) Kosmulski, M., *Chemical Properties of Material Surfaces*; Marcel Dekker: New York, 2001; p 753.
(70) Norde, W. *J. Dispersion Sci. Technol.* **1992**, *13*, 363–377.
(71) He, Y.; Hower, J.; Chen, S.; Bernards, M. T.; Chang, Y.; Jiang, S. *Langmuir* **2008**, *24*, 10358–10364.
(72) Zheng, J.; Li, L. Y.; Chen, S. F.; Jiang, S. Y. *Langmuir* **2004**, *20*, 8931–8938.
(73) Zheng, J.; Li, L. Y.; Tsao, H. K.; Sheng, Y. J.; Chen, S. F.; Jiang, S. Y. *Biophys. J.* **2005**, *89*, 158–166.
(74) Feng, W.; Zhu, S. P.; Ishihara, K.; Brash, J. L. *Langmuir* **2005**, *21*, 5980–5987.
(75) Su, T. J.; Lu, J. R.; Thomas, R. K.; Cui, Z. F.; Penfold, J. *J. Phys. Chem. B* **1998**, *102*, 8100–8108.
(76) Norde, W. *Colloids Surf., B* **2008**, *61*, 1–9.
(77) Norde, W., *Colloids and Interfaces in Life Sciences*. Dekker: New York, 2003.
(78) Leavis, P. C.; Rothstei., F *Arch. Biochem. Biophys.* **1974**, *161*, 671–682.
(79) Qin, G.; Cai, C. *Chem. Commun.* **2009**, 5112–4.
(80) Sharma, S.; Johnson, R. W.; Desai, T. A. *Langmuir* **2004**, *20*, 348–356.
(81) Sofia, S. J.; Premnath, V.; Merrill, E. W. *Macromolecules* **1998**, *31*, 5059–5070.